A simple model for friction detachment at an interface of finite size mimicking Fineberg's experiments on uneven loading

A. Papangelo[1], B. Stingl[2], N.P. Hoffmann[2,3], M. Ciavarella[1]

[1]Politecnico di Bari, [2]Hamburg University of Technology, [3]Imperial College London

Abstract: This work presents a model and simulation results for the friction detachment of a finite sized interface, following previous results on the phenomenon by Ben-David and Fineberg (Ben-David & Fineberg, [1]), namely "*experiments demonstrating that the ratio of shear to normal force needed to move contacting bodies can, instead, vary systematically with controllable changes in the external loading configuration".*

In particular, we extend a previous one-dimensional simulation model by Bar Sinai et al. [2,3] to a quasi 2D model to allow for a tilting of one of the contacting blocks. While Bar Sinai et al [2,3] postulate that the presence of "slow fronts" of detachment (1 order of magnitude lower than the usual Rayleigh fronts as in crack propagation) is due to a strengthening term in the friction law (Bar Sinai et al [2,3]), which is not always measured in unlubricated contacts, we find slow fronts also with a purely weakening law.

1. Introduction

The basic laws of (dry) friction seem simple and have apparently been understood centuries ago by the Italian scientist Leonardo and the French engineers Coulomb and Amontons: the frictional force between two bodies in static contact is proportional to the normal force. The constant of proportionality is called ‘coefficient of (static) friction’. This surprisingly simple law, independent on the macroscopic shape of the body and the apparent area of contact, has been interpreted first by Bowden and Tabor in Cambridge [4] as due to the fact that the contact occurs only on microscopic asperities and the pressure locally is sufficient to cause yield - friction is therefore due to asperity junction plastic failure, and the friction coefficient is the ratio between shear strength and hardness, i.e. about 3 times the yield strength of the softer material (this is the so called ‘ploughing term’, and there can be also an adhesion contribution). Later on, statistical models explained that the average pressure on each asperity tends to be constant, and only the number of contacting asperities changes with increasing normal force. Greenwood and Williamson [5] confirmed the proportionality of contact area and normal force with such a statistical approach. Hence, what happens on the asperity scale is crucial to friction.

When sliding starts, thermal effects are activated, both at bulk and asperity scales, and this is usually one of the factors called upon to explain the rate-dependence of friction as part of the difference between static and dynamic friction coefficient (see Rice, [6]). Yet, for many scopes, the Coulomb law is still very much in use, and more complicated laws are often developed empirically trying to account for the influence of other factors, such as speed, normal load, surface conditions, temperature, etc. (see Rabinovicz, [7]). To summarize, while the basic law is still useful for very qualitative results, the understanding of frictional processes is still very far from even remotely completed.

Dieterich [8] and Ruina [9], see also Dieterich [10], suggested a rate- and state-dependent friction law to explain a large amount of laboratory data on rock friction. The state variable quantifies the contact state between sliding surfaces or the internal structure of the gouge layer between sliding surfaces. Various empirical forms exist which consider interface strength as a dynamic entity that is inherently related to both fast processes such as detachment/re-attachment, and the slow process of contact area rejuvenation. This can be put as an extension of Bowden and Tabor's model, which states the solid friction force F needed to slide one solid against the other at relative velocity V reads: $F = \sigma \Sigma$, with Σ the total real area of contact, and σ the shear strength within microcontacts. For low velocities, the variations of the friction force are governed by the competition between two effects in the two terms of the equation (σ, Σ), which can be separately treated:

a) Geometric aging: asperities creep plastically, and Σ increases quasi-logarithmically with contact duration Φ, the "geometric age". When motion starts, contacts get gradually destroyed, after age Φ, and replaced by new ones. When the interface sits still, it ages (strengthens); when it slides, it rejuvenates (and hence weakens, according to this first criterion). This incidentally causes a static friction peak by loading at constant velocity.
b) Velocity dependence of the sliding strength σ: for many interfaces increasing strength is found (similar to lubrication, but in dry friction it is a rheology resulting from thermally activated "depinning" dissipative events occurring within the adhesive joint).

It is this second term which shows crucially important in explaining the transient from rest to motion. Until recently, there was only indirect measurement of all these effects of contact area size at asperity scale, and no detailed information about the space-time evolution of the contact area and stresses along the interface.

Fineberg experiments on PMMA

Recently, an interesting series of experiments has been conducted by the group of Jay Fineberg in Israel, based on a new measurement technique (Rubinstein et al [11]). In their experiments, they use two blocks of transparent material (PMMA, poly methyl-methacrylate), permitting real-time visualization of the net contact area that forms the interface separating two blocks of like material. The underlying idea is that by illuminating with a very small angle to the surface, only the areas in contact can transmit the light across the interface, and hence, the change in contact area can be detected optically. Hence, sliding is seen indirectly as a "change of contact area", but notice that, for a given normal load, we would expect the contact area to stay

globally constant. These studies are showing a complex pattern of propagating fronts at the interface, where the fast fronts (subsonic and intersonic) are very similar to those expected from classical theories of fracture mechanics. The third type of front, an order of magnitude slower, was found to be the dominant mechanism for the rupture of the interface, since sliding occurs only when one such slow front traverses the entire interface. Indeed, slow fronts are responsible for the most significant redistribution of stress (due to the local change of contact area), whereas fast fronts are too fast to alter the state of the interface. The resulting apparent friction coefficient depends very much on the details of the dynamical processes of these alternating slow and fast fronts, and these in turn strongly depend on the loading and geometrical conditions. In more recent experiments (Ben-David and Fineberg [8]), Fineberg's group varied the stress profiles across the interface by a small tilting of the top block (one or two hundredths of a degree). They found a large variation on the apparent friction coefficient with different loading states and normal forces, and they observed different details of the dynamics of the rupture leading to relative motion.

The only other experiment of the type of Fineberg in Israel has been attempted in Japan, by the group of Ken Nakano (see Maegawa et al [12]). With a simple serial block model they did explain how the apparent static friction coefficient can be less than the nominal static friction coefficient due to the residual strain in the slider, and a difference between static and dynamic friction coefficient. However, a careful look at the experiment shows that they seem to have different results on the contact area reduction during sliding --- Nakano's group has a large 30%, whereas Fineberg group had only just 10%, despite the experiments seem on the same material, PMMA. In addition we note that Maegawa et al [12] do not report a dependency of the static friction coefficient on the applied normal stress distribution. However, comparing figures 4, 6 and 7 in their publication a slight dependency can be observed.

Early attempts of interpreting slow fronts

The slow fronts have been tentatively explained by a Burridge-Knopoff spring-block type model (Braun et al [13]), introducing some appropriate statistical distribution of the stiffness and rupture thresholds of the surface contacts, as well as time delays to reattach broken contacts. They found that for moderately flexible surface contacts, an excess stress develops at the tip of the arrested Rayleigh fronts, which can trigger a slow detachment front, representing the motion of individual blocks, whose properties determine the front speed.

In a recent 2D block model (Trømborg et al [14]) with standard Coulomb friction (but with difference in a static and dynamic friction coefficient) a few results obtained by the experiments are reproduced. In particular, that front speed depends strongly on both the instantaneous stresses and the friction coefficients, through a non-trivial scaling parameter. However: (i) they do not seem to find the slow fronts - the slowest front was about a fourth of Rayleigh speed - still an order of magnitude faster than Fineberg's slow fronts (ii) and they have a different scaling of speed vs excess stress, less universal. On the other hand, there is no real reduction of apparent friction. Another interesting recent paper is that of Scheibert and Dysthe [15], which shows with a minimal quasistatic 1D model, how a very small "tilting" in Fineberg's experiments can affect

the kinematics of the transition from static friction to stick-slip motion. The analysis in a sense corresponds to that predicted decades ago by Cattaneo and Mindlin [16, 17, 18] using Amontons' law of friction. Here, however, the "full stick" solution is considered to be uniform shear distribution (avoiding to discuss edge effects), whereas the pressure is "tilted" by the effect of the tangential force, which is applied to a certain height of the specimen. Below a certain height (and in particular, for the tangential force aligned with the interface), no precursor is observed.

Bouchbinder model using friction strengthening

Recently, the blocks model of Braun et al [13], has been extended to a continuous model by Bouchbinder and coworkers [2,3,19], who have obtained a set of interesting results. Confirming the findings of Braun et al [13], with a mesoscopic model of friction containing evolution laws for the contact area and for the "elastic" contribution term in friction, they seem to explain most of the findings by Fineberg. In particular, it was shown that Fineberg's slow fronts are an intrinsic and robust property of simple non-monotonic rate-and-state friction laws (Heslot et al, [20], Kilgore et al, [21]). In other words, they suggest they occur with strenghtening friction laws, associated with a new velocity scale c_{min}, intrinsically determined by the friction law, below which steady state rupture cannot propagate. Ruptures hence occur in a continuum of states, from c_{min} to elastic wave-speeds, as found experimentally.

In the present paper, we shall attempt another approach to the explanation of the slow fronts and in general of the Fineberg's results --- paying attention to the effect which was considered most relevant in the latest contributions from Finberg's group, namely the tilting of the pad. Our research was motivated by studies on the sticking to sliding transition in disc brakes ([22]), where the influence of the tilting on the detachment process was observed. In this work we present numerical simulations using our disc brake model using PMMA parameters.

2. The model

We consider an elastic block between two rigid plates, as schematically described in Fig.1.This model set up is a generic representation of a sliding system with dry friction and was even used for some numerical investigations on the brake pad-disk contact [22]. (This is why some terminology is taken from the brake system field)

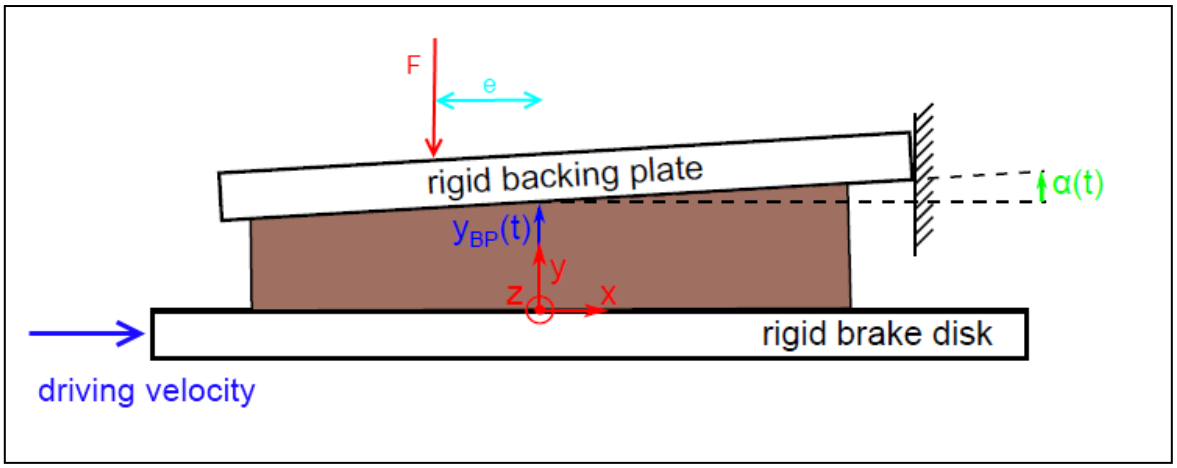

Figure 1: The model of a sliding pad between two rigid plates.

Here we summarize the key-features of the model:

- Rigid backing plate;
- Rigid brake disc;
- Plane strain condition;
- Lining material isotropic and linear elastic;
- Free edges;
- Small deformations;
- Absence of wear.

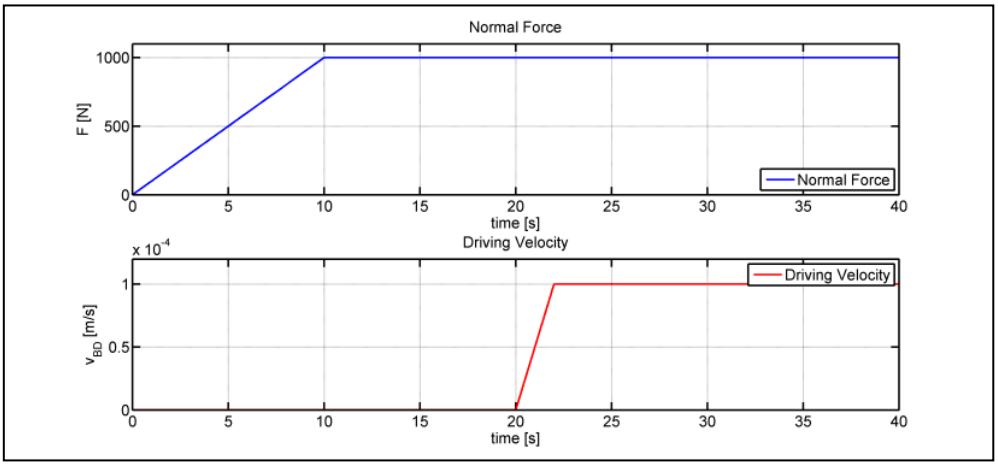

Figure 2: The loading trajectories on normal force and driving velocity.

Following Bar-Sinai et al [3] we integrated the equation of motion for the x direction along y to obtain a reduction of the problem from 2D to 1D where we took the rigid body motion of the backing plate into account (see the appendix for the complete derivation). The final equation of motion is:

$$\rho H \frac{\partial^2 u(x,t)}{\partial t^2} = \frac{2G}{1-\bar{\nu}} H \frac{\partial^2 u(x,t)}{\partial x^2}\left(1+\frac{\bar{\nu}^2}{1-2\bar{\nu}}\right) + \\ +G\alpha(t)\left(1+\frac{2\bar{\nu}}{1-2\bar{\nu}}\right) - \frac{2Gu(x,t)}{H} + \tau_{fric}(x,t) - c\frac{\partial u}{\partial t}(x,t), \quad (1)$$

where *u(x,t)* is an average, in the y direction, of the displacement of the lining material in the x direction. On the left hand side one can find the inertial term, while the right hand side terms express the contribution of the stresses σ_{xx} and σ_{xy}. τ_{fric} is the frictional stress and c represents a numerical damping in the system.

The frictional stress was obtained using Bouchbinder's model [2,3,16] with the frictional stress

$$\tau_{fric} = \tau^{\mathrm{el}} + \tau^{\mathrm{vis}} = \tau^{\mathrm{el}} + \eta\, v^*\, A\, \mathrm{sgn}(v_{rel}) \ln\left(1+\frac{|v_{rel}|}{v^*}\right), \quad (2)$$

the evolution equations for the elastic frictional stress

$$\frac{\partial \tau^{\mathrm{el}}}{\partial t} = \frac{\mu_0 A}{h} v_{rel} - \frac{\tau^{\mathrm{el}}|v_{rel}|}{D}\,\vartheta\left(\frac{|\tau|}{A}-\tau_c\right), \quad (3)$$

and for the contact age φ

$$\frac{\partial \varphi}{\partial t} = 1 - \frac{\varphi\,|v_{rel}|}{D}\,\vartheta\left(\frac{|\tau|}{A}-\tau_{\mathrm{c}}\right). \quad (4)$$

The real area of contact

$$A(\sigma_{yy},\varphi) = A_0\left[1+b\ln\left(1+\frac{\varphi}{\varphi_0}\right)\right] \quad (5)$$

is given by the contact age and the pressure dependent un-aged contact area

$$A_0 = \left.\frac{|\sigma_{yy}|}{\sigma_H}\right|_{x,0,t}. \quad (6)$$

In the above equations "v_{rel}" is the relative velocity between the elastic material and brake disk, "σ_{yy}" is the normal pressure at the interface, while the others quantities are listed and described in the table 1.
To study the detachment process we apply the normal force with a linear increase from 0 to F_{max} in the first 10 seconds; after some rest of 10 seconds to give to the system the possibility to reach the equilibrium, we increase the velocity of the brake disc with a linear ramp from 0 to v_{max} in the time interval from 20 to 22 s; the velocity of the disc and the force are then kept constant. These loading trajectories are shown in Figure 2.

After each simulation we computed the static friction coefficient from the interface stresses by

$$f_{st} = \max\left[\frac{p\int_0^L \tau_{fri}(x,y=0)dx}{p\int_0^L \sigma_{yy}(x,y=0)dx}\right], \quad (7)$$

where L is the length of the pad and p is its depth, respectively 200 mm and 120 mm.

The sign of the eccentricity is taken coherent with the x-axis and in the following sections it is computed as $\frac{e}{L/2}$.

3. Results

We ran simulations using the parameters of the sketched geometry and for the material PMMA as listed in the Tab. 1 taken from [3]:

DESCRIPTION	SYMBOL	VALUE	UNITS
Elastic shear modulus	G	3100	MPa
Poisson's modulus	$\bar{\nu}$	0,35	1
Density	ρ	1200	kg/m^3
Mean size of contacts	D	0,5	mm
Shear strength	τ_c	130	MPa
Hardness	σ_H	540	MPa
Viscous friction coefficient	η	27	MPa (s/µm)
reference scale of velocity	v^*	0,1	µm/s
b coefficient	b	0,075	1
reference temporal scale	φ_0	3,33*10^{-4}	s
ratio (interfacial stiffness)/(effective height of the asperities)	μ_0/h	300,0	MPa/µm
Pad height	H	15	mm
Pad length	L	200	mm
Pad depth	p	120	mm
Tilt angle	α	/	rad

Table 1- Geometry and PMMA parameters.

With the model and the loading described above we ran a large numerical parameter study varying the eccentricity, the normal force and the brake disc velocity. All the simulated sticking to sliding transitions share some common features: the detachment process starts from one edge and transverses through the whole interface. This detachment front can generally be subdivided into three parts.

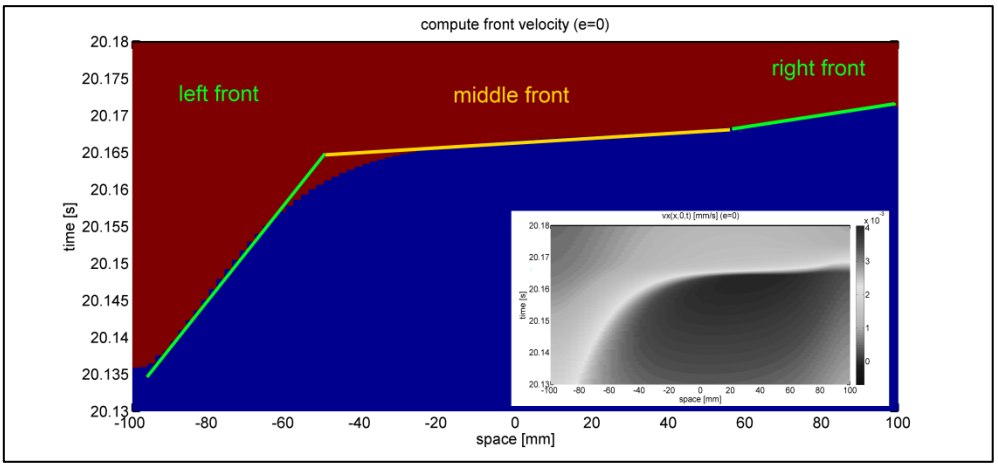

Figure 3: Detachment front originating from the left edge: A slow precursor exists for the first 55mm (left front), followed by the faster intermediate (middle) front. Closer to the trailing edge from +55mm on the slower right front can be observed. The blue area indicates points with a velocity above 40% of the maximum velocity reached during this detachment process; the velocity of the red points is below this arbitrarily chosen but characteristic threshold which has been introduced to visualize the detachment front. On the bottom right hand corner the dynamical process without labels and in greyscale is reported. (For this particular case *e=0*).

As an example we take the detachment process obtained when the normal force is applied in the middle of the backing plate (i.e. *e=0*). As shown in Figure 3 the detachment process starts with a slow precursor originating at the left which accelerates to the middle front at approximately -45mm and slows down again at approximately +55mm to the slower right front. However, depending on the parameters, the left and the right front do not always exist, while the middle detachment front is a robust feature of the system. As shown in the following, we will discuss the dependency of the static friction coefficient on the external loading and its relation to the interface dynamics sketched above.

Figure 4 shows the increase of the friction coefficient moving the normal force from the leading to the trailing edge. The difference between the highest and the lowest value of the static friction coefficient with respect to the mean value is around the 0,5%. While this variation is small with respect to the observations by Fineberg's group [1], we observe the same trend: the friction coefficient is higher for a tilting to the trailing edge.

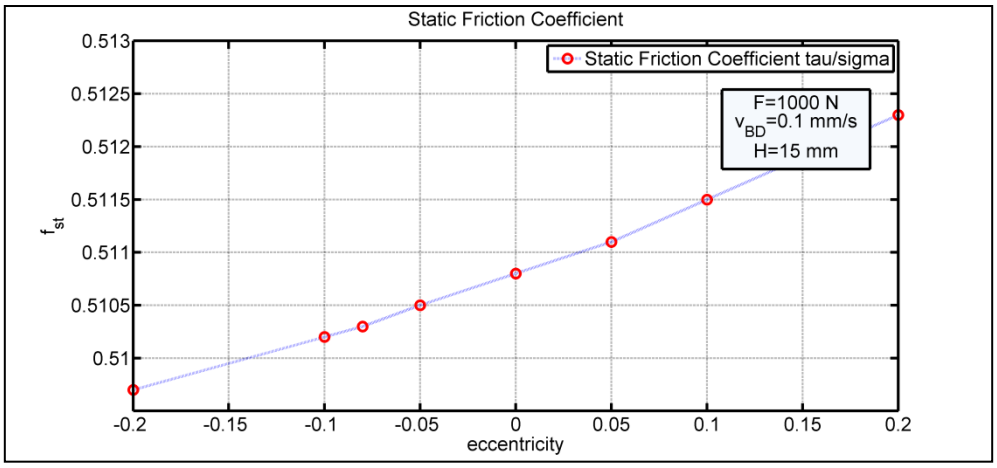

Figure 4: Dependency of the static friction coefficient on the eccentricity.

Varying the normal force, the static friction coefficient seems to saturate to a limit value for high forces as shown in Figure 5 where we collected the value of the static friction coefficient for zero eccentricity.

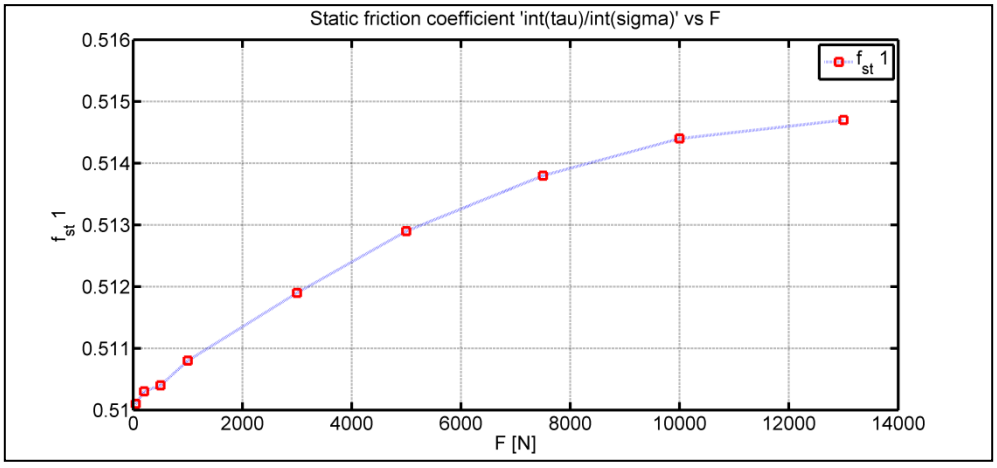

Figure 5: The static friction coefficient as a function of the normal force for zero eccentricity.

Connecting the variation of the friction coefficient with the interface dynamics two interesting relations were found. Figure 6 reports a linear dependency between the static friction coefficient and the velocity of the left precursor front. In addition to the velocity, the static friction also depends linearly on the length of the left precursor, as shown in Figure 7. The latter linear relation coincides with the results found by Otsuki and Matsukawa [23]. However, the underlying physics are different, as for Otsuki and Matsukawa the linear instability of the quasistatic precursor leads to a rapid front while in our system the whole detachment process is quasistatic as discussed below.

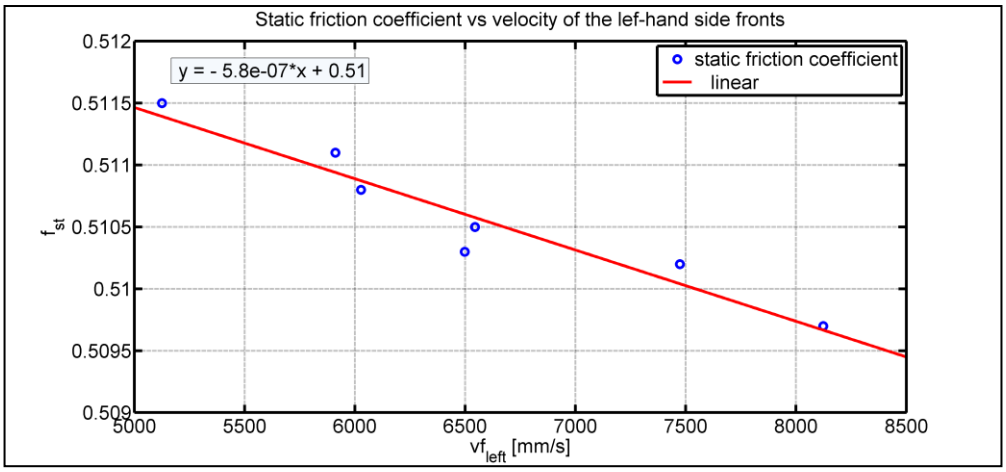

Figure 6: Static friction coefficient as a function of the left precursor velocity. The detachment events shown here share a normal force of 1000N but were observed for different eccentricities.

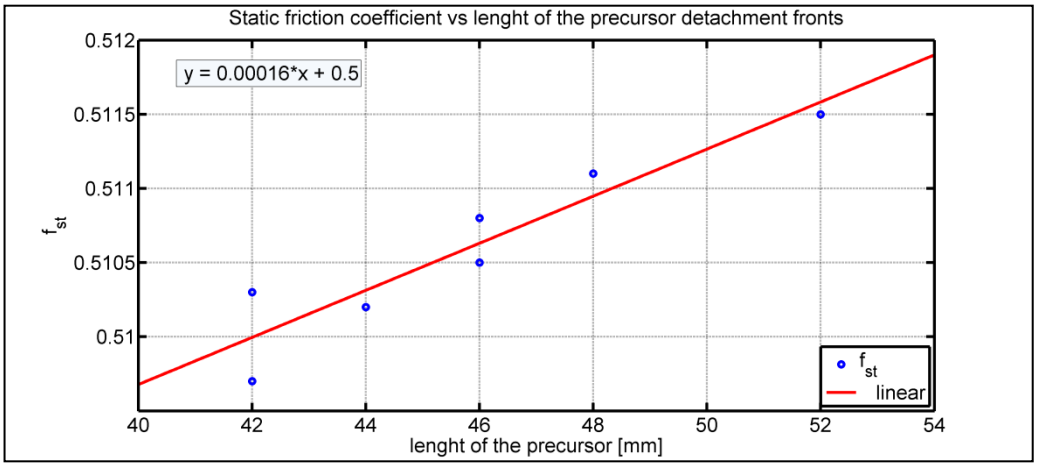

Figure 7: Static friction coefficient vs. the length of the left precursor. The events shown are the same as in Figure 6.

This overall behaviour was found for the value of the normal force equal to 1000 N and 5000 N, while for lower normal forces the detachment process does not include the left precursor front.

The order of magnitude of the velocity of the detachment fronts is close to the slow fronts reported in the literature, except for the left precursor fronts that seem even slower, see Figure 8. Looking to the normal force dependency of the front velocities the right front differs from the other two: While for the middle fronts and for the left hand side fronts the front velocity diminishes increasing the magnitude of the normal force, the right hand side fronts seem to maintain a constant average velocity for all the values of eccentricity. The lower detachment velocity could be related to the bigger influence of the friction when the normal force is higher. We plotted the reciprocal of the velocity of the left hand side fronts against the value of the normal force. The result is reported in Figure 9 and shows a clear linear relationship between the above-mentioned variables. To sum up, the velocity of the precursors seems to be in inverse proportion with respect to the normal force applied.

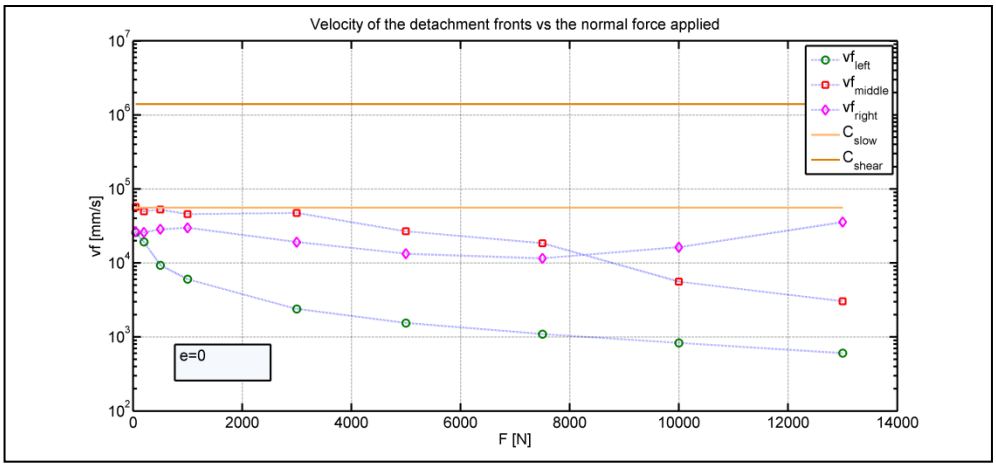

Figure 8: velocity of the left, middle and right front vs. the normal force, compared to the shear wave speed and the speed of the slow fronts reported in [2].

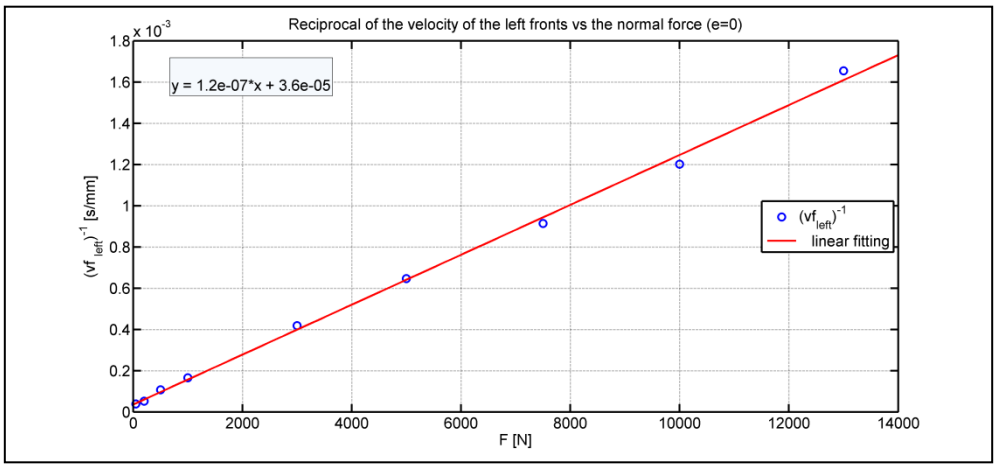

Figure 9: Linear relationship between the inverse of the left precursor velocity and the normal force.

The left, middle and right detachment fronts increase their velocity when the driving velocity v_{BD} is increased. This kind of relationship is also reported by Otsuki and Matsukawa [23]. Plotting the velocity of the fronts with respect to the driving velocity in a double-logarithmic diagram the curve approaches a line as shown in Figure 10 for a normal force of 500 N and zero eccentricity. This common feature suggests that our detachment fronts are quasistatic, just as the precursors observed by Otsuki and Matsukawa.

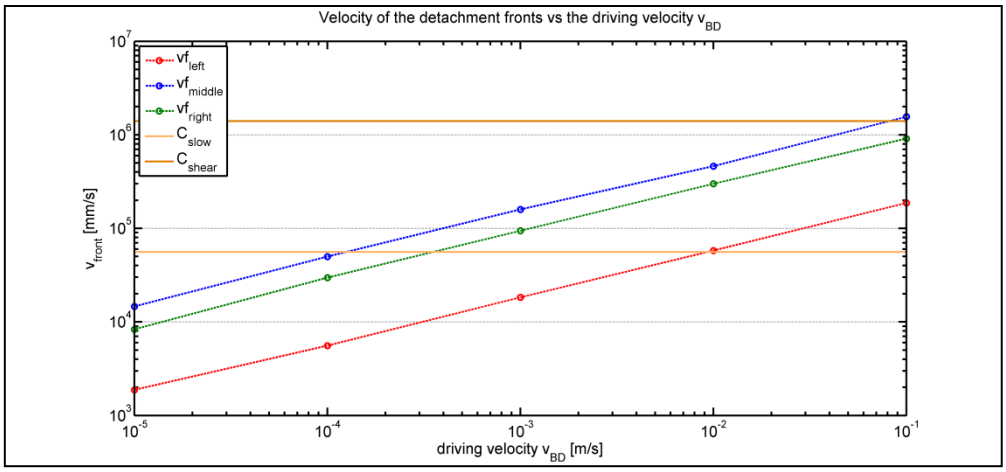

Figure 10: Dependency of the left, middle and right front velocity on the driving velocity for 500N and zero eccentricity.

We test this hypothesis by suddenly stopping the disc during the detachment phase. Figure 11 shows the velocity of the friction material along the sample against the time. At 20.15 s we suddenly stopped the disc and all the dynamics at the interface stopped synchronously. These results support the idea that the fronts are indeed quasi-static and do not possess an intricate inner or local dynamics.

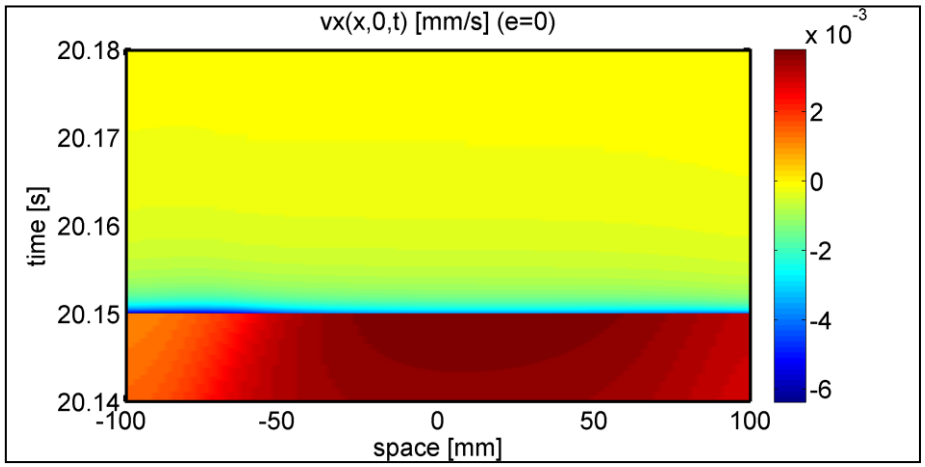

Figure 11: Velocity field of the pad for a sudden stop of the disc during the detachment process at 20.15s.

We finally close our discussion with a numerical experiment on the contribution of the velocity strengthening part of the friction law. We eliminated the strengthening branch from the friction law setting the viscous friction coefficient η equal to 0 and ran simulations measuring the velocity of the detachment fronts. Figure 12 compares the velocity of the fronts with and without strengthening. As one can see the velocity of the fronts seems to be not influenced by the strengthening branch. This is an interesting result as the velocity of the slow fronts was reported to depend on the minimum of the steady state friction coefficient. However, eliminating the strengthening branch this minimum vanishes. Potentially the tilting degree of freedom in our model – which is generic for any sliding system of finite length – is a crucial contribution to

the detachment process. The importance of this friction induced torque resulting in a tilted pressure distribution in the interface has e.g. already been discussed in [15].

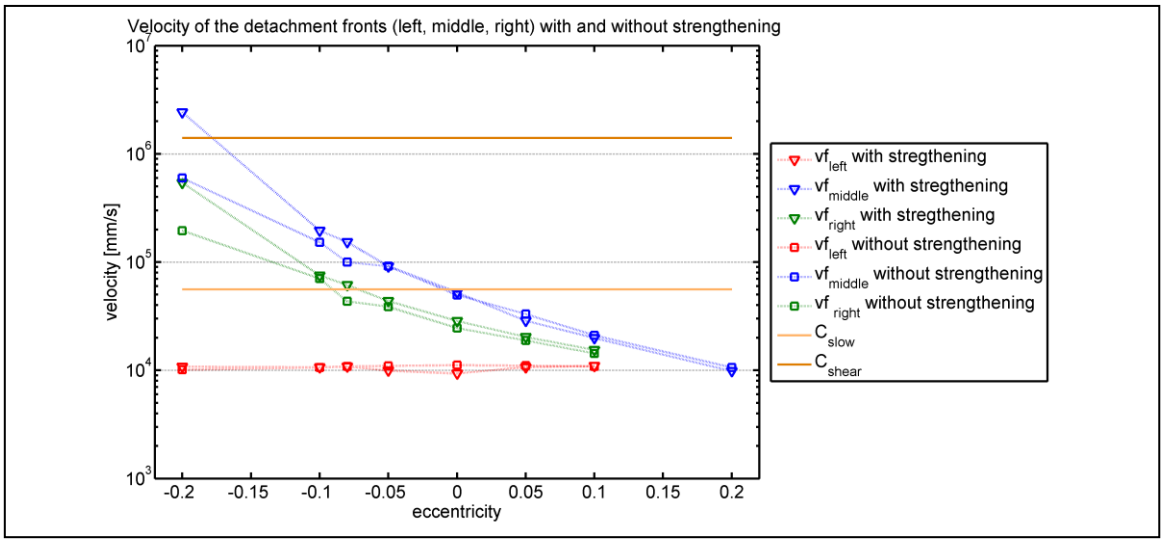

Figure 12: Influence of the velocity strengthening branch in the friction law on the velocities of the left, middle and right front, plotted here against the eccentricity.

The velocity strengthening term does, however, have a marked effect on the overall system level static friction coefficient. Figure 13 shows the static friction coefficient as a function of the driving velocity. Plotted in a semi-logarithmic diagram the static friction coefficient increases linearly with the disc velocity. We believe that this behaviour is linked to the strengthening branch of the static friction coefficient. To check this hypothesis we set the viscous friction coefficient to 0 and again evaluated the behaviour of the static friction coefficient with respect to the driving velocity (see Figure 14). In this case a higher driving velocity results in a lower static friction coefficient until a limit value is reached. This kind of behaviour can be due to the effect of the aging. When the driving velocity is low the detachment takes longer than in the case with high driving velocity. Thus the aging of the contact area becomes important and yields to an increase of the static friction coefficient.

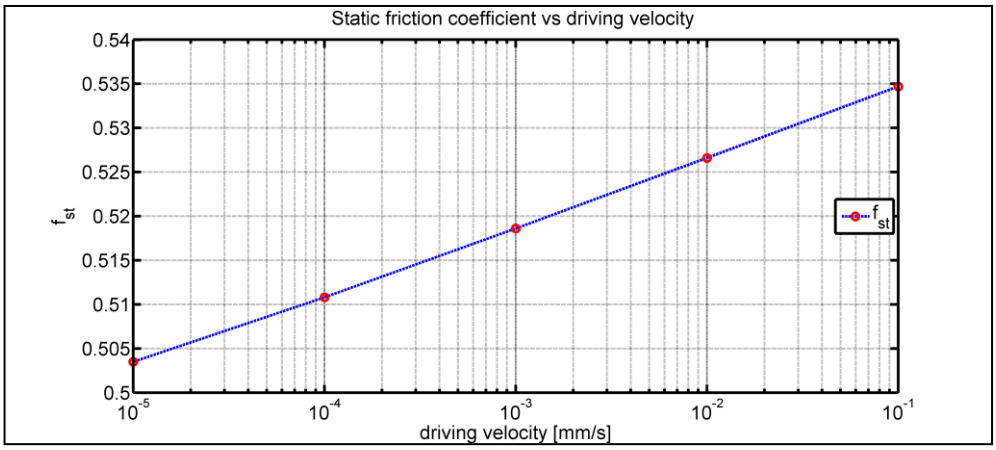

Figure 13: Dependency of the static friction coefficient on the driving velocity with the velocity strengthening contribution in the friction law.

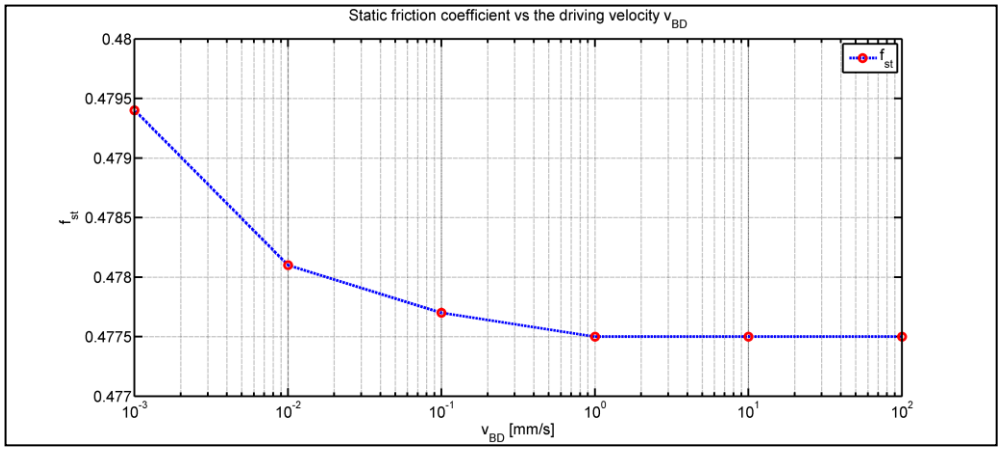

Figure 3: Dependency of the static friction coefficient on the driving velocity without the velocity strengthening contribution in the friction law.

4. Summary and Conclusions

To our knowledge this work is the first to give numerical confirmation of Fineberg's experimental results [2] on the effect of asymmetric normal loading. While the observed variation of the friction coefficient is rather small we were able to identify clear relationships between the precursor fronts and the macroscopic friction coefficient. Especially the influence of the precursor length coincides with previous results ([23]), although the underlying mechanism may be of different nature. Nevertheless Fineberg's experimental results ([1]) show that the precursor length decreases when the static friction coefficient increases which is indeed opposite in our results. The origin of this contrary finding might be in the loading geometry: Fineberg applies a homogeneous shear load along the interface while Otsuki considers edge loading. The coincidence of our results - obtained with a homogeneous loading - with Otsuki's edge loading system is probably due to our simplified continuum mechanics description as discussed below.

The detachment fronts found in our studies are quasistatic and independent on the minimum of the steady state friction coefficient. Nevertheless, our model was able to predict the intensively discussed slow fronts semiquantitively. However, we stress that this result may be due to the strong simplifications in our model which were introduced by the one dimensional approximation of the two dimensional continuum. This leads to a lack of vertical dynamics as the only vertical degree of freedom is given by the rigid body motion of the backing plate. We believe that the approximation error is especially large at the edges. E.g. our model does not allow for lift off at the edges of the interface – a process that might have a tremendous effect on the nucleation of detachment fronts. Extension of the present model to capture full 2D continuum dynamics of the pad is thus a topic of ongoing and future studies.

ACKNOWLEDGEMENTS

The authors are thankful to Yohai Bar Sinai for his helpful comments on the reduction from 2D to 1D.

REFERENCES

[1] O. Ben-David, & J Fineberg, Static Friction Coefficient Is Not a Material Constant , J. Phys.Rev. Lett. 106, 254301. (2011)

[2] Y. Bar-Sinai, R. Spatschek, E. Brener, E. Bouchbinder On the velocity-strengthening behaviour of dry friction arxiv 1308.1420 (2013)

[3] Y. Bar Sinai, E. A. Brener, and E. Bouchbinder. Slow rupture of frictional interfaces, Geophys. Res. Lett., 39, L03308, 2011. (2012)

[4] F. P. Bowden, and D. Tabor, The friction and lubrication of solids, part I. Oxford: Clarendon Press. 1950

[5] J. A. Greenwood and J. B. P. Williamson, Contact of Nominally Flat Surfaces, Proc. R. Soc. Lond. A vol. 295 no. 1442 300-319. (1966)

[6] J.R. Rice, Heating and weakening of faults during earthquake slip. J. Geophys.Res. 111, B05311, doi:10.1029/2005JB004006. (2006).

[7] E. Rabinovicz, Friction and wear of materials, John Wiley & Sons, New York. 1995

[8] J.H.Dieterich, Modeling of rock friction 1. Experimental results and constitutive equations. J. Geophys. Res. 84, 2161-2168. (1979).

[9] A.L.Ruina, Slip instability and state variable friction laws. J. Geophys. Res. 88,10359-10370. (1983).

[10] J.H. Dieterich Applications of Rate- and State-Dependent Friction to Models of Fault Slip and Earthquake Occurrence, Treatise on Geophysics, 2007, Chapter 4.04, Pages 107-129. (2007)

[11] SM. Rubinstein G Cohen & J Fineberg Detachment fronts and the onset of dynamicfriction, Nature 430, 1005-1009. (2004).

[12] S Maegawa, A Suzuki and K Nakano, Precursors of Global Slip in a Longitudinal Line Contact Under Non-Uniform Normal Loading , Tribology Letters 38(3), 313-323. (2010)

[13] Braun, O. M. , Barel, I. , and Urbakh, M. Dynamics of Transition from Static to Kinetic Friction, Phys. Rev. Lett. 103, 194301, (2009)

[14] J. Trømborg, J. Scheibert, DS Amundsen, K Thøgersen, and A Malthe-Sørenssen, Transition from static to kinetic friction: Insights from a 2D model, Phys. Rev. Lett. 107, 074301. (2011)

[15] J. Scheibert and DK Dysthe Role of friction-induced torque in stick-slip motion, EPL 9254001 doi: 10.1209/0295-5075/92/54001 (2010)

[16] C Cattaneo, Sul contatto di due corpi elastici: Distribuzione locale degli sforzi. Rendiconti dell'Accademia nazionale dei Lincei, 27, 342-248, 434-436, 474-478. (1938)

[17] R. D., Mindlin, "Compliance of Elastic Bodies in Contact," J. Applied Mechanics Trans. ASME, 16, pp. 259-268. (1949)

[18] Mindlin, R. D., and Deresiewicz, H., "Elastic Spheres in Contact Under Varying Oblique Forces," J. Applied Mechanics Trans. ASME, 20, pp. 327-344. (1953)

[19] E. Bouchbinder, T. Goldman, J. Fineberg The Dynamics of Rapid Fracture: Instabilities, Nonlinearities and Length Scales arxiv 1305.0989. (2013)

[20] F Heslot, T. Baumberger, B. Perrin, B. Caroli, and C. Caroli, Creep, stick-slip, and dry friction dynamics: Experiments and a heuristic model, Physical Review E, 49 (6), 497-4988. (1994)

[21] BD Kilgore, ML Blanpied, and JH Dieterich, J. H., Velocity dependent friction of granite over a wide range of conditions, Geophysical Research Letters, 20 (10), 903-906. (1993)

[22] S Kruse et al, The influence of loading conditions on the static coefficient of friction – a study on brake creep groan, submitted to IMAC XXXII (2014)

[23] Michio Otsuki & Hiroshi Matsukawa (2013), Systematic breakdown of Amontons' law of friction for an elastic object locally obeying Amontons' law, Nature, Scientific Reports 3, Article number: 1586 doi:10.1038/srep01586